Dynamics of the Self-Assembly of Unilamellar Vesicles

T. M. Weiss,[1] T. Narayanan,[1,*] C. Wolf,[2] M. Gradzielski,[2,†] P. Panine,[1] S. Finet,[1] and W. I. Helsby[3]

[1]*European Synchrotron Radiation Facility, BP 220, F-38043 Grenoble Cedex, France*
[2]*Lehrstuhl für Physikalische Chemie I, Universität Bayreuth, D-95440 Bayreuth, Germany*
[3]*Daresbury Laboratory, Cheshire, WA4 4AD, United Kingdom*

We have studied the transient stages in the formation of unilamellar vesicles with millisecond time resolution. The self-assembly was initiated by rapid mixing of equimolar amounts of anionic and zwitterionic micelles and the transient micellar entities were probed by time-resolved small-angle x-ray scattering. Within the mixing time, original micelles transformed to disklike micelles which evolved further to a critical size and then closed to form monodisperse unilamellar vesicles within a second. Subsequent growth led to an unexpected broadening of the vesicle size distribution.

The equilibrium microstructure of a large number of surfactant systems has been widely studied over the past several decades [1,2]. Depending on concentration, temperature and other physicochemical parameters, a variety of structures such as spherical, cylindrical or disklike micelles, bicelles, vesicles, and lamellar, cubic and hexagonal phases have been identified [1–4]. The transient intermediate structures formed during the transition between two equilibrium phases have come to be the focus of attention only recently [5–12]. The micelle to vesicle transition is the classic example [3], where the final vesicle phase can be a long-lived metastable state in lieu of the equilibrium lamellar phase [7,12]. The rapid structural transitions can be conveniently induced by mixing two different micellar solutions in the millisecond time scale [5,9]. Recently, the formation of vesicles has been studied *in situ* but the exact route remains unclear though disklike intermediate states have been inferred [9,10,12]. Understanding the dynamical behavior of micellar self-assembly is primordial in exploiting the self-assembling properties of amphiphilic system in applications such as encapsulation, controlled release, and nanoreactors [13]. However, the time scales of the underlying structural organization may range from a millisecond up to weeks [3,14] and the very early transient micellar entities remained inaccessible for structural studies.

In this Letter, we report millisecond time-resolved small-angle x-ray scattering (SAXS) study of micelle to vesicle transition in a novel zwitterionic-anionic micellar mixture. The results revealed a transient state consisting of disklike micelles which grew during the initial few hundred milliseconds and then closed to form unilamellar vesicles with a narrow size distribution.

Equimolar (50 mM) amounts of zwitterionic and anionic solutions were mixed in a stopped-flow apparatus (Biologic, SFM-3). The dead time of the mixing and the transfer to the scattering capillary cell (diameter 1.6 mm quartz and wall thickness ~10 μm) was less than 4 ms. Data acquisition was triggered at the beginning of the mixing phase that continued for 15 ms and then ceased by a solenoid stopper. During this time the mixture was in a quasicontinuous flow corresponding to a constant kinetic time ($t < 4$ ms).

The time-resolved SAXS experiments were performed at the ID2 beam line [15] of the European Synchrotron Radiation Facility (ESRF) in Grenoble, France. Most of the SAXS measurements were made using the RAPID gas detector [16] loaned from the Daresbury Laboratory in the United Kingdom. The high brilliance of the source together with a state-of-the-art photon counting detector provided sufficient intensity statistics with an acquisition time of 1 ms. Additional measurements were performed using an image intensified charge-coupled device (CCD) detector [15] to probe the vesicle formation and their final state. The data presented here are averaged over 5 ms for the initial growth and 50 ms at the later stages. The measured two dimensional scattered intensities were treated using the standard procedure [15] to obtain the azimuthally averaged, normalized intensities as a function of scattering vector, $q[= (4\pi/\lambda)\sin(\theta/2)]$, with λ the wavelength of incident beam ($=0.996$ Å) and θ the scattering angle. The background scattering of the stopped-flow cell filled with water was then subtracted and the resulting quantity is denoted by $I(q)$.

The time-resolved scattered intensities were analyzed using the scattering function, $P(q, R)$, of monodisperse objects (disks or spherical shells) with radius (R) weighted by a Schulz size distribution, $f(R)$ [17]. The resulting expression for the polydisperse case has the following general form,

$$I(q) = N \int_0^\infty P(q, R)f(R)dR, \qquad (1)$$

where N is the number density of scatterers, and $f(R)$ is given by

$$f(R) = \left(\frac{Z + 1}{R_m}\right)^{Z+1} \frac{R^Z}{\Gamma(Z + 1)} \exp\left(-\frac{Z + 1}{R_m}R\right), \qquad (2)$$

with R_m is the mean radius, and the polydispersity is characterized by $Z + 1 = 1/p^2$, where p is the polydispersity index $[p^2 = (\langle R^2 \rangle / R_m^2) - 1]$. For disklike objects p refers only to the radius, and the bilayer thickness (H) is assumed to be uniform. For randomly oriented disks of radius R and thickness H, $P(q, R, H)$ is given by the following expression [17] involving the first order Bessel function J_1,

$$P(q, R, H) = V^2 \Delta\rho^2 \int_0^{\pi/2} \left\{ \left[\frac{2J_1(qR\sin\phi)}{qR\sin\phi} \right] \times \left[\frac{\sin((qH/2)\cos\phi)}{(qH/2)\cos\phi} \right] \right\}^2 \sin\phi \, d\phi, \quad (3)$$

where $V(= \pi R^2 H)$ is the volume of the disk, $\Delta\rho^2 = (\rho_B - \rho_S)^2$ with ρ_B and ρ_S the scattering length densities of the bilayer and the solvent, respectively, and ϕ is the orientation angle.

For spherical shell-like objects, $P(q, R)$ can be expressed [17] in terms of the scattering amplitudes of two spheres of radii R_1 and R_2,

$$P(q, R_1, R_2) = 16\pi^2 \Delta\rho^2 \{R_2^3 f_0(qR_2) - R_1^3 f_0(qR_1)\}^2, \quad (4)$$

where $f_0(x) = (\sin x - x\cos x)/x^3$ is the scattering amplitude of a solid sphere and $R_2 - R_1$ is the bilayer thickness.

The surfactant mixtures were comprised of zwitterionic tetradecyldimethylamine oxide $[C_{14}H_{29}N(CH_3)_2O]$ and anionic lithium perfluorooctanoate $(C_7F_{15}COOLi)$. Both surfactants were gifts by Clariant (Germany) and purified by repeated recrystallization from acetone and CCl_4, respectively. The fluorinated chains provided a higher contrast for x-ray scattering experiments. The initial zwitter-ionic micelle (M_1) has short rodlike shape with radius 1.85 nm and length 15 nm (aggregation number 320) at the given concentration [18,19], while the anionic perfluoro micelle (M_2) is spherical with radius 1.0–1.2 nm and average aggregation number 36 [20]. Figure 1 displays the $I(q)$ from an equimolar mixture of zwitterionic (M_1) and anionic (M_2) micelles within the first 5 ms after mixing (including the dead time). For a comparison, $I(q)$'s from the original micelles are also shown, which over this q range is primarily dominated by the micellar form factor (except at small q range). The continuous lines for M_1 and M_2 correspond to rod and sphere fits, respectively, but the fitted radius of the rods (M_1) is relatively smaller (≈ 1.49 nm) presumably due to the very low x-ray contrast of the their head groups in water. Evidently the original micelles transformed to a new shape within the mixing time. $I(q)$ at the very beginning can be adequately described by Eqs. (1) and (3) corresponding to disklike objects with a radius 7.5 nm and a thickness 4.8 nm, which is bigger than the estimated bilayer thickness of 3.9 nm (twice the length of the stretched tetraalkylchains). Furthermore, the observed size corresponds to a surfactant aggregation number of 670, about twice the aggregation number of the original M_1 rodlike micelles. This indicates that the initial mixed micelles may have formed from one M_1 micelle and the corresponding number of perfluoro micelles to attain equimolar composition. Figure 2 shows the growth of mixed micelles with time (t). The continuous lines correspond to Eqs. (1) and (3) with a radius polydispersity index 0.2 and demonstrate the existence of disklike intermediates in this self-assembly process. The fit tends to deviate around 400 ms, suggesting the formation of new structures.
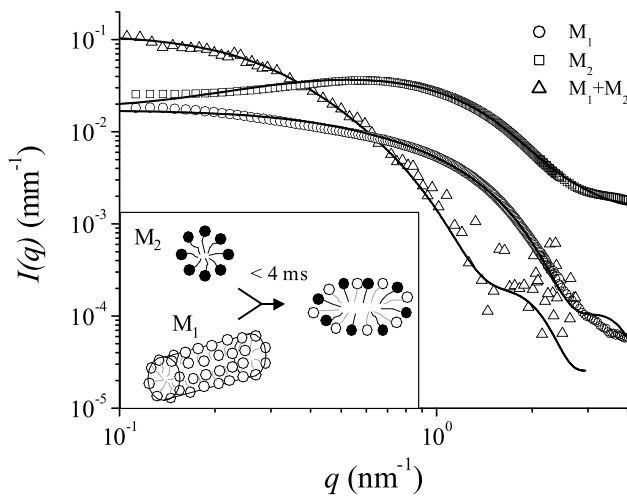
FIG. 1. SAXS intensities for 50 mM solutions of $C_{14}H_{29}N(CH_3)_2O$ (M_1) and $C_7F_{15}COOLi$ (M_2) together with their mixture within the first 5 ms after rapid mixing. The continuous line for the mixture ($M_1 + M_2$) corresponds to polydisperse disk scattering function. The inset schematically depicts the corresponding micellar transformation.
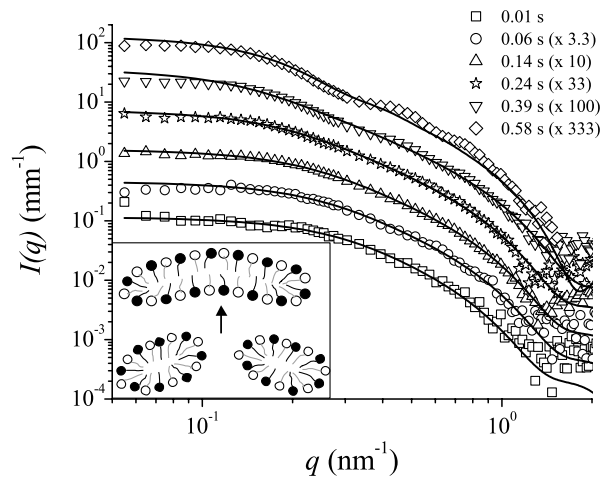
FIG. 2. The evolution of $I(q)$ indicating the growth of disklike micelles over the first few hundred milliseconds after mixing. The solid lines are fits to Eqs. (1) and (3) with polydispersity index $= 0.2$ ($t < 0.5$). For clarity, successive curves have been multiplied by the factor indicated in parentheses. The inset is a cartoon of the underlying growth process.

The time evolution of disk radius and thickness is depicted in Fig. 3. During the growth process, H decreased to the expected value (3.6 nm) and R increased by an exponential function. The continuous line represents

$$R = R_M\left[1 - \frac{R_M - R_0}{R_M}\exp(-t/\tau)\right], \qquad (5)$$

with R_M the final radius, R_0 the radius of initially formed disks at $t = 0$, and $1/\tau$ the growth rate. The exponential time dependence depicted in Eq. (5) is the signature of a growth process from metastable state [21]. The driving mechanism is very likely the unfavorable edge energy arising from the packing constraints characterized by the line tension Λ [10,12]. To reduce the edge energy, the floppy micelles coalesce until they reach a critical radius denoted by R_M.

The observed growth rate ($1/\tau \approx 5\ \mathrm{s}^{-1}$) is orders of magnitude smaller than that expected for a purely diffusive process at the given concentration and size ($1/\tau \approx 7800\ \mathrm{s}^{-1}$). This together with the exponential time dependence suggests a reaction-limited process [22]. The floppy micelles have to make several attempts before joining to form a larger micelle—presumably in an edge-to-edge conformation.

Figure 4(a) shows the transformation of the floppy micelles to unilamellar vesicles. At intermediate times (400–800 ms), $I(q)$ is not adequately described by either Eq. (3) or (4). This is due to a coexistence of disklike micelles and closed vesicles. Figure 4(b) illustrates the formation of the vesicles and their growth obtained from an additional experiment using the CCD detector. The long time behavior of the vesicles ($\sim 4.5 \times 10^6$ s) depicted in Fig. 4(b) is derived from a separate *ex situ* experiment. The continuous lines in Figs. 4(a) and 4(b) are fits to Eqs. (1) and (4) illustrating the formation of vesicles with a narrow size distribution within a few seconds, as demonstrated by the well-

defined fringes in $I(q)$. The deviation at low q is due to the repulsive structure factor of the charged vesicles [17,23]. After a certain induction period (~ 30 s), the monodisperse vesicles grow further as indicated by the shift in the first minimum in $I(q)$ to smaller q values. While the radius (R_V) increased from 13 to 28 nm in about 600 s, the polydispersity index showed an unexpected increase from 0.1 to 0.29. The broadening of the size distribution is vividly demonstrated by the gradual diminishing of oscillations in $I(q)$, which is likely due to the tendency of larger vesicles to coalesce. The time dependence of radius ($t > 30$ s) is consistent with a power law, $R_V \sim t^{1/3}$, which together with the observed single size distribution suggests that the growth mechanism is reminiscent of a coalescence process governed by diffusion [24].

FIG. 3. Time dependence of the disk radius (R) and thickness (H). The continuous line pertains to the exponential function in Eq. (5) with $R_M = 15.1$ nm, $R_0 = 6.6$ nm, and $\tau = 198$ ms.
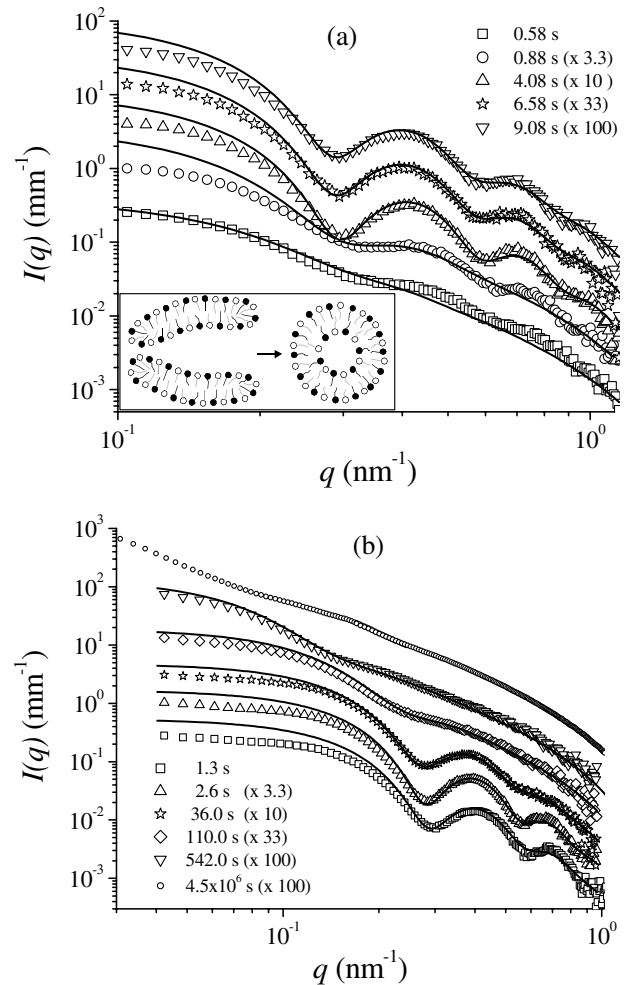
FIG. 4. Transformation of floppy micelles to unilamellar vesicles and the subsequent growth. The solid lines are fits to spherical shell using Eqs. (1) and (4). (a) Inset schematically depicts the transformation. (b) The radius of the shell increased from 13.2 nm (1.3 s) to 27.2 nm (542 s) and the polydispersity increased from 0.106 to 0.29. For clarity, successive curves have been multiplied by the factor indicated in parentheses.

The vesiculation depends on the balance between the unfavorable edge energy ($2\pi R\Lambda$) of the disks and the bending energy required to form spherical structures which is determined by the mean bending modulus κ and the saddle-splay modulus $\bar{\kappa}$ of the amphiphilic bilayer [8,10,12]. Above a critical radius ($\approx R_M$) disklike micelles become energetically unstable and this marks the onset of vesicle formation. From the energy balance [8] the maximum disk radius $R_M \sim 4(2\kappa + \bar{\kappa})/\Lambda$, whereas the measured $R_M \sim 15$ nm. Therefore, the ratio $(2\kappa + \bar{\kappa})/\Lambda \sim 3.8$ nm, which is very reasonable since other experiments yielded $2\kappa + \bar{\kappa} \sim 3$–$5k_BT$ and $\Lambda \sim k_BT/$nm [8,10,12].

The fact that the initial R_V (~13 nm) is comparable to R_M (~15 nm) suggests that the incipient vesicles are formed from the closure of objects which in turn resulted from the fusion of two disks of radius just below R_M. These newly formed objects with radius in the range $R_M < R < \sqrt{2}R_M$ are energetically unstable (e.g., spherical caplike intermediates) [10], and they close to form vesicles with half the radius. The narrow size distribution of the vesicles at the early stages is an indication of the sharpness of this energy balance. The polydisperse vesicles formed at late stages remain unilamellar and stable for months, as indicated by the upper curve in Fig. 4(b) (final $R_V \approx 50$ nm). This increase of polydispersity is significantly different from that observed in mixtures of cationic and anionic surfactants where the final state has the sharpest size distribution [9]. This difference may be attributed to weaker attractive interaction in the zwitterionic-anionic mixture. The energetic stabilization of a well-defined curvature of the bilayer by attractive electrostatic interactions is a key factor for the stability [8] of monodisperse unilamellar vesicles that is significantly less pronounced in zwitterionic-anionic (interaction parameter of $-12k_BT$) than in catanionic surfactant mixtures ($-21k_BT$).

The above results demonstrate that transformation of micelles to vesicles is a multistep process. The tendency for surfactant pairing and the comprehensive equimolar mixing play a crucial role in the formation of initial floppy micelles. The millisecond time resolution permitted probing the early stages of micelle-vesicle transition, most notably the growth and transformation of floppy micelles to vesicles. The measurement of the initial vesicle size constitutes a good method to determine the ratio of the mechanical moduli of surfactant bilayers which is not easily accessible by other techniques. Millisecond time-resolved SAXS is a powerful method to elucidate fast structural dynamics in soft matter systems. The transient structural properties of these complex systems can be exploited in engineering hierarchically ordered nanostructured materials [25].

*Corresponding author.
Email address: narayan@esrf.fr
†Present address: Technische Universitaet Berlin, D-10623 Berlin, Germany.
Email address: michael.gradzielski@tu-berlin.de

[1] R. G. Laughlin, *The Aqueous Phase Behavior of Surfactants* (Academic, San Diego, 1994).
[2] *Micelles, Membranes, Microemulsions, and Monolayers*, edited by W. M. Gelbart, A. Ben-Shaul, and D. Roux (Springer-Verlag, New York, 1994).
[3] E. W. Kaler *et al.*, Science **245**, 1371 (1989).
[4] T. Zemb *et al.*, Science **283**, 816 (1999).
[5] A. J. O'Connor, T. A. Hatton, and A. Bose, Langmuir **13**, 6931 (1997).
[6] S. U. Egelhaaf and P. Schurtenberger, Phys. Rev. Lett. **82**, 2804 (1999).
[7] K. Horbaschek, H. Hoffmann, and J. Hao, J. Phys. Chem. B **104**, 2781 (2000).
[8] H.-T. Jung *et al.*, Proc. Natl. Acad. Sci. U.S.A. **98**, 1353 (2001); Proc. Natl. Acad. Sci. U.S.A. **99**, 15 318 (2002).
[9] S. Schmoelze *et al.*, Phys. Rev. Lett. **88**, 258301 (2002).
[10] A. Shioi and T. A. Hatton, Langmuir **18**, 7341 (2002).
[11] H. Wang *et al.*, Phys. Rev. E **67**, 060902(R) (2003).
[12] J. Leng, S. U. Egelhaaf, and M. E. Cates, Biophys. J. **85**, 1624 (2003).
[13] M.-P. Pileni, Nat. Mater. **2**, 145 (2003); J. Patarin, B. Lebeau, and R. Zana, Curr. Opin. Colloid Interface Sci. **7**, 107 (2002).
[14] E. A. G. Aniansson and S. N. Wall, J. Phys. Chem. **78**, 1024 (1974).
[15] T. Narayanan, O. Diat, and P. Bösecke, Nucl. Instrum. Methods Phys. Res., Sect. A **467**, 1005 (2001).
[16] R. A. Lewis *et al.*, Nucl. Instrum. Methods Phys. Res., Sect. A **392**, 32 (1997).
[17] J. S. Pedersen, in *Neutrons, X-Rays and Light: Scattering Methods Applied to Soft Condensed Matter*, edited by P. Linder, and T. Zemb (Elsevier, Amsterdam, 2002), p. 391.
[18] H. Hoffmann, G. Oetter, and B. Schwandner, Prog. Colloid Polym. Sci. **73**, 95 (1987).
[19] N. Gorski and J. Kalus, J. Phys. Chem. B **101**, 4390 (1997).
[20] M. Gradzielski, I. Grillo, and T. Narayanan, Prog. Colloid Polym. Sci. 129, 32 (2004).
[21] K. Binder and P. Fratzl, in *Phase Transformations in Materials*, edited by G. Kostorz (Wiley-VCH, Weinheim, 2001), p. 411.
[22] R. C. Ball *et al.*, Phys. Rev. Lett. **58**, 274 (1987).
[23] *Modern Aspects of Small-Angle Scattering*, edited by H. Brumberger (Kluwer, Dordrecht, 1995).
[24] D. Beysens, Y. Garrabos, and C. Chabot, in *Slow Dynamics in Complex Systems*, edited by M. Tokuyama and I. Oppenheim (AIP, New York, 1999), p. 222.
[25] H. P. Hentze *et al.*, Langmuir **19**, 1069 (2003).